

Title: An Exact Map Between the TBG (and multilayers) and Topological Heavy Fermions, Andrei Bernevig, Princeton University

Speakers:

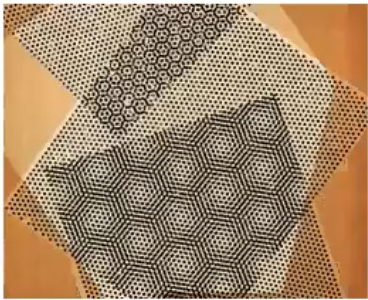
Series: Quantum Matter

Date: March 28, 2022 - 12:00 PM

URL: <https://pirsa.org/22030026>

Abstract: Magic-angle ($\approx 1.05^\circ$) twisted bilayer graphene (MATBG) has shown two seemingly contradictory characters: the localization and quantum-dot-like behavior in STM experiments, and delocalization in transport experiments. We construct a model, which naturally captures the two aspects, from the Bistritzer-MacDonald (BM) model in a first principle spirit. A set of local flat-band orbitals (f) centered at the AA-stacking regions are responsible to the localization. A set of extended topological conduction bands (c), which are at small energetic separation from the local orbitals, are responsible to the delocalization and transport. The topological flat bands of the BM model appear as a result of the hybridization of f - and c -electrons. This model then provides a new perspective for the strong correlation physics, which is now described as strongly correlated f -electrons coupled to nearly free topological semimetallic c -electrons - we hence name our model as the topological heavy fermion model. Using this model, we obtain the $U(4)$ and $U(4) \times U(4)$ symmetries as well as the correlated insulator phases and their energies. Simple rules for the ground states and their Chern numbers are derived. Moreover, features such as the large dispersion of the charge ± 1 excitations and the minima of the charge gap at the $\nu = 0$ point can now, for the first time, be understood both qualitatively and quantitatively in a simple physical picture. Our mapping opens the prospect of using heavy-fermion physics machinery to the superconducting physics of MATBG. All the model's parameters are analytically derived.

MATBG = Topological Heavy Fermion



Zhida Song



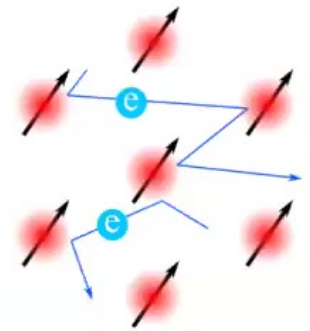
Jonah H. Arbeitman



Aaron Chew



Fang Xie



TBG at 2 Pi Flux: arXiv:2111.11434, arXiv:2111.11341



Ali Yazdani



Dmitry Efetov



Biao Lian



Oskar Vafek



Nicolas Regnault

https://bank.gov.ua/en/

← → ↻ https://bank.gov.ua/en/ ☆ 🛡️ ⬇️ 📄 🌐 ☰



[About](#) [Consumer protection](#) [For people with visual impairments](#) | [Ua](#)
[Monetary Policy](#) [Financial Stability](#) [Supervision](#) [Payments and Settlements](#) [Financial Markets](#) [Statistics](#) [Hryvnia](#) [News](#)



Support the Armed Forces of Ukraine and People Affected by Russia's Aggression

Підтримати Збройні Сили України та постраждалих від російської агресії

THE ARMED FORCES >

HUMANITARIAN AID >

Card number
.....

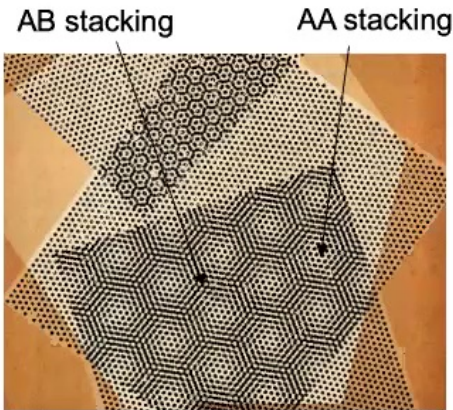
Expiration CVV2
MM/YY ... ?

By pressing the button «Pay» you accept [Terms and conditions](#)

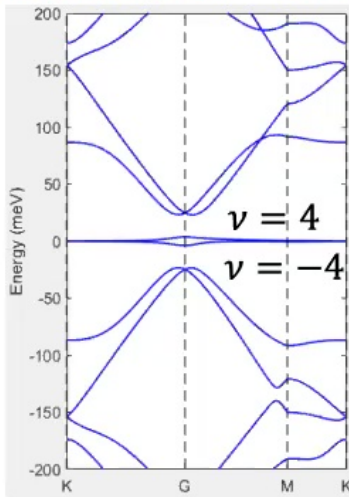
Pay



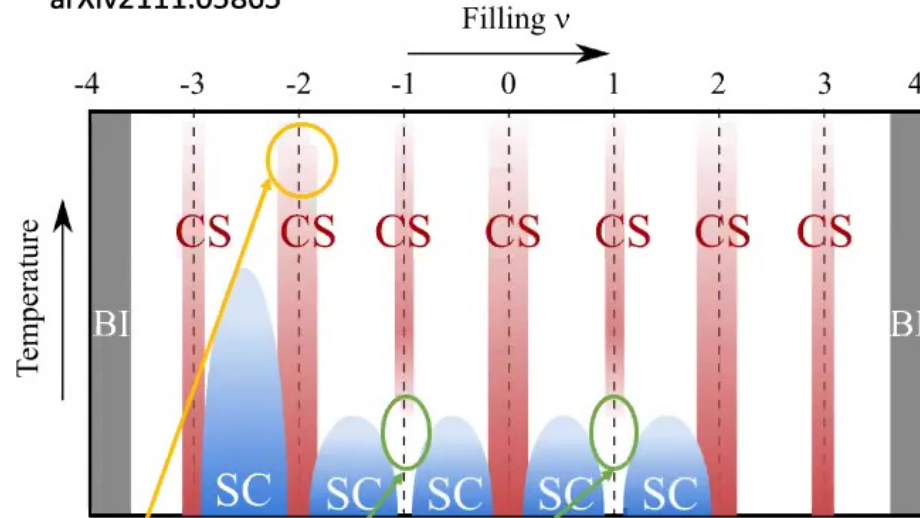
Experimental facts



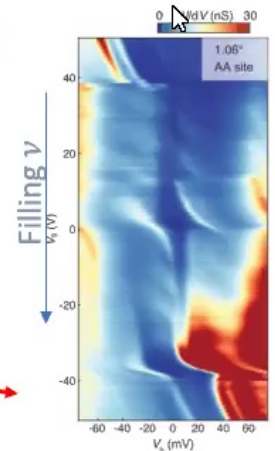
Magic angle $\theta = 1.05^\circ$



Bistritzer, MacDonald 2011PNAS

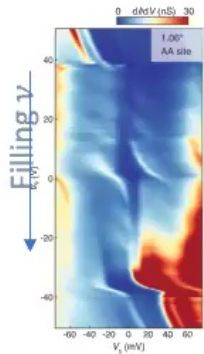


1. **Correlated insulator or correlated states (CS)** Cao et al. 2018, Lu et al. 2019, Sharpe et al. 2019, Saito et al. 2020, Stepanov et al. 2020, Wong et al. 2020, Choi et al. 2019, Kerelsky et al. 2019, Jiang et al. 2019
 2. **Chern insulator** Serlin et al. 2019, Nuckolls et al. 2020, Choi et al. 2020, Saito et al. 2021, Das et al. 2021, Park et al. 2021, Wu et al. 2021,
 3. **Superconductivity (SC)** Cao et al. 2018, Lu et al. 2019, Yankowitz et al. 2019, Saito et al. 2020, Stepanov et al. 2020
 4. **Strange metal** Cao et al. 2020, Polshyn et al. 2019
 5. **Pomeranchuk effect** Saito et al. 2021, Rozen et al. 2021
 6. **Dirac-like behavior** Zondiner et al. 2020, Saito et al. 2021, Rozen et al. 2021
 7. **Quantum-dot-like behavior** Wong et al. 2020, Xie et al. 2019, Choi et al. 2019, Kerelsky et al. 2019, Jiang et al. 2019
- others...

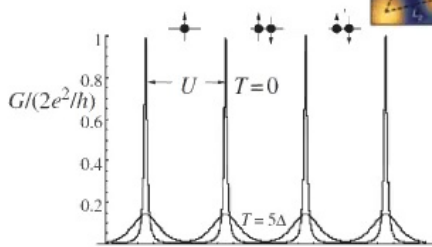


Experiments suggesting existence of *local moments*

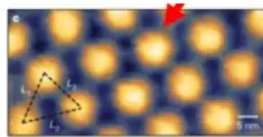
Coulomb blockade seen in STM



→ large on-site repulsion



Xie2019, Choi2019, Kerelsky2019, Jiang2019, Wong2020



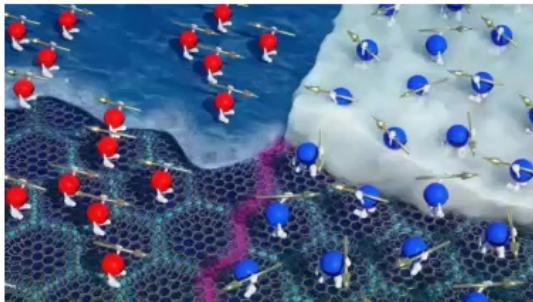
contradictory in conventional picture



Pomeranchuk effect

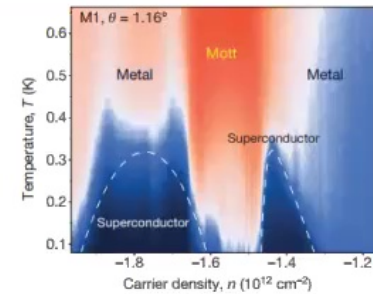
large entropy in the ordered phase, which disappear under magnetic field → loosely coupled local moments

Saito2021, Rozen2021

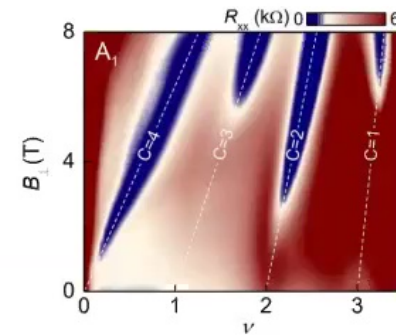


Experiments suggesting existence of *delocalized electron states*

Metallicity & Superconductivity



Landau fans



Transport & Hysteresis, Efetov group 2020

Zondiner2020

Dirac-like behavior

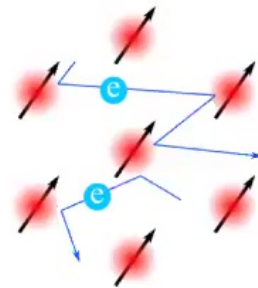
“Dirac revivals” near transition point, where compressibility $\sim \sqrt{n}$

Is topological flat-band
the answer to the
contradictory?

A phenomenological
model would consist of
both local moments &
itinerant electrons

topology \rightarrow delocalized wave function

flatness \rightarrow "localization"?



relation?

Heavy Fermion Physics?

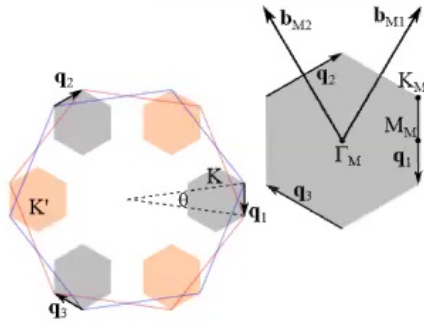
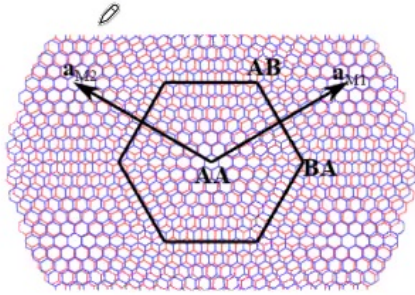
This work: **EXACT** mapping between MATBG and a heavy fermion model

- All parameters are calculated in a *first-principle* way
- Most numerical results are explained
- Insights into new physics, Pomeranchuk, SC, etc

- **Construction of our model**
- *New understanding of correlated states*
- *Insight into new physics*



Fragile and stable topology



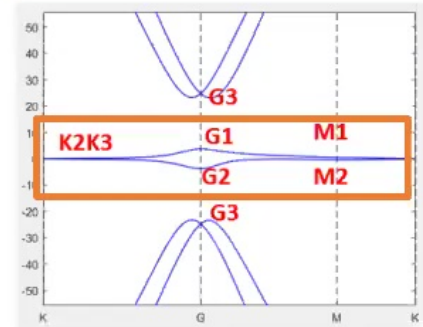
Crystalline symmetries in a single valley

- MSG 177.151 P6'2'2 ← C3z, C2zT, C2x
- Valley-U(1)
- Time-reversal

Bistritzer MacDonald 2011PNAS

Fragile topology

Song2019PRL, Po2019PRB, Liu2019PRB



Bistritzer2011PNAS

	Γ_1	Γ_2	Γ_3	M_1	M_2	K_1	K_2K_3
E	1	1	2	E	1	1	E 1 2
$2C_3$	1	1	-1	C_2'	1	-1	C_3 1 -1
$3C_2'$	1	-1	0				C_3^{-1} 1 -1

Band representations (local orbitals)

Bradlyn2017Nature, Po2017NC

Elcoro2021NC: we derive all magnetic BRs & topological indices

Wyckoff pos.	$1a$ (000)			$2c$ ($\frac{1}{3}\frac{2}{3}0$), ($\frac{2}{3}\frac{1}{3}0$)		
Site sym.	$6'22', 32$			$32, 32$		
EBR	$[A_1]_a \uparrow G$	$[A_2]_a \uparrow G$	$[E]_a \uparrow G$	$[A_1]_c \uparrow G$	$[A_2]_c \uparrow G$	$[E]_c \uparrow G$
Orbitals	s	p_z	p_x, p_y	s	p_z	p_x, p_y
Γ (000)	Γ_1	Γ_2	Γ_3	$2\Gamma_1$	$2\Gamma_2$	$2\Gamma_3$
K ($\frac{1}{3}\frac{1}{3}0$)	K_1	K_1	K_2K_3	K_2K_3	K_2K_3	$2K_1 \oplus K_2K_3$
M ($\frac{1}{2}00$)	M_1	M_2	$M_1 \oplus M_2$	$2M_1$	$2M_2$	$2M_1 \oplus 2M_2$

→ Obstruction to two-band symmetric & local lattice models

Two-band models where C2zT becomes nonlocal

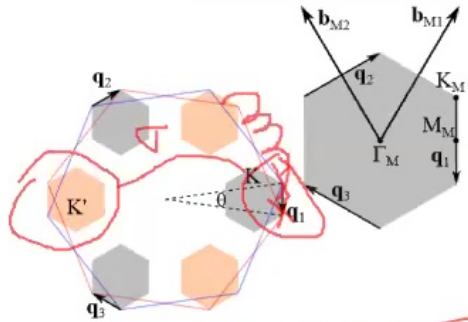
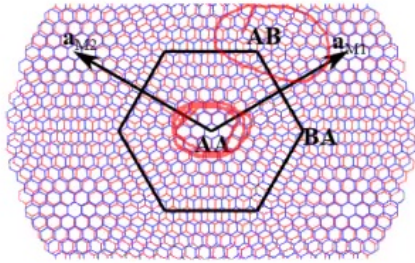
Kang2018PRX, Kang2019PRL, Koshino2018PRX, Yuan2018PRB

(Fragile) topology

Song2019PRL, Po2019PRB

See Song2020Science for generic criteria for fragile states.

Fragile and stable topology



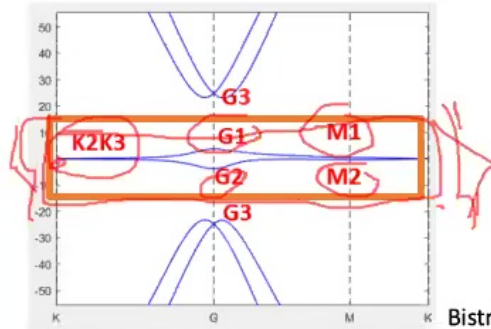
Crystalline symmetries in a single valley

- MSG 177.151 $P6'2'2 \leftarrow C3z, C2zT, C2x$
- Valley-U(1)
- Time-reversal

Bistritzer MacDonald 2011PNAS

Fragile topology

Song2019PRL, Po2019PRB, Liu2019PRB



Bistritzer2011PNAS

	Γ_1	Γ_2	Γ_3	M_1	M_2	K_1	K_2K_3
E	1	1	2	E	1	1	E
$2C_3$	1	1	-1	C_2'	1	-1	C_3
$3C_2'$	1	-1	0				C_3^{-1}

Band representations (local orbitals)

Bradlyn2017Nature, Po2017NC

Elcoro2021NC: we derive all magnetic BRs & topological indices

Wyckoff pos.	$1a$ (000)			$2c$ $(\frac{1}{3}\frac{2}{3}0), (\frac{2}{3}\frac{1}{3}0)$		
Site sym.	$6'22', 32$			$32, 32$		
EBR	$[A_1]_a \uparrow G$	$[A_2]_a \uparrow G$	$[E]_a \uparrow G$	$[A_1]_c \uparrow G$	$[A_2]_c \uparrow G$	$[E]_c \uparrow G$
Orbitals	s	p_z	p_x, p_y	s	p_z	p_x, p_y
Γ (000)	Γ_1	Γ_2	Γ_3	$2\Gamma_1$	$2\Gamma_2$	$2\Gamma_3$
K $(\frac{1}{3}\frac{1}{3}0)$	K_1	K_1	K_2K_3	K_2K_3	K_2K_3	$2K_1 \oplus K_2K_3$
M $(\frac{1}{2}00)$	M_1	M_2	$M_1 \oplus M_2$	$2M_1$	$2M_2$	$2M_1 \oplus 2M_2$

→ Obstruction to two-band symmetric & local lattice models

Two-band models where $C2zT$ becomes nonlocal

Kang2018PRX, Kang2019PRL, Koshino2018PRX, Yuan2018PRB

(Fragile) topology

Song2019PRL, Po2019PRB

See Song2020Science for generic criteria for fragile states.

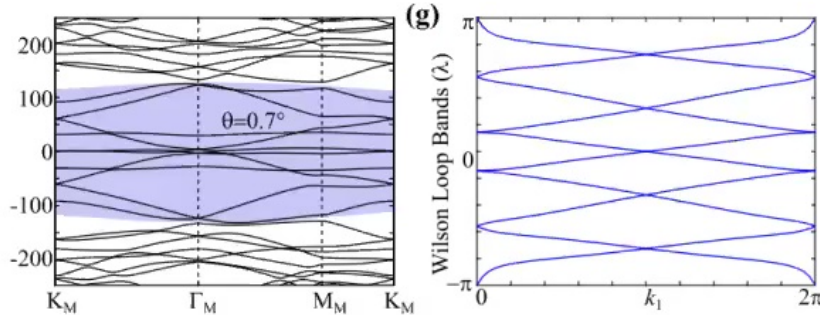
Fragile and stable topology

Stable topology

\mathbf{P} ($E_k = -E_{-k}$) is an emergent particle-hole symmetry of the BM continuous model

Song2021PRB TBG-II

Reflected as charge-conjugation symmetry in experiments

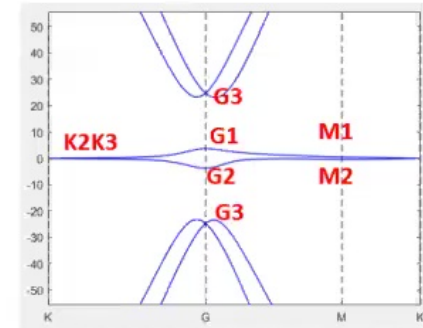
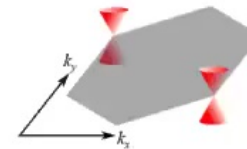


Wilson loop

$$W(k_x) = T \exp \left(i \int dk_y \cdot A(k_y) \right)$$

Non-abelian berry's connection

We further prove that $4n+2$ ($n \in \mathbb{N}$) Dirac points \leftrightarrow Topology



Symmetry Anomaly

→ forbids symmetric & short-range lattice models with any finite number of bands

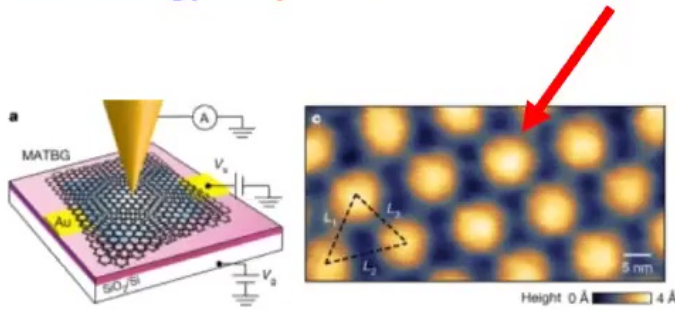
Two-band models where $C2zT$ becomes nonlocal *Kang2018PRX, Kang2019PRL, Koshino2018PRX, Yuan2018PRB*

Ten-band model where P becomes nonlocal *Po2019PRB*

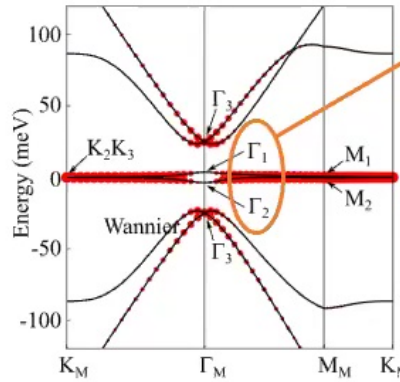


Construction of the heavy fermion model

Our strategy: **Step I. Where does the local states come from?**



Xie2019, Choi2019, Kerelsky2019, Jiang2019, Wong2020



Suppose we can replace $\Gamma_1 + \Gamma_2$ by Γ_3 , then flat bands match p_x, p_y orbitals at triangular lattice

Wyckoff pos.	1a (000)		
Site sym.	$6'22', 32$		
EBR	$[A_1]_a \uparrow G$	$[A_2]_a \uparrow G$	$[E]_a \uparrow G$
Orbitals	s	p_z	p_x, p_y
$\Gamma (000)$	Γ_1	Γ_2	Γ_3
$K (\frac{1}{3} \frac{1}{3} 0)$	K_1	K_1	$K_2 K_3$
$M (\frac{1}{2} 00)$	M_1	M_2	$M_1 \oplus M_2$

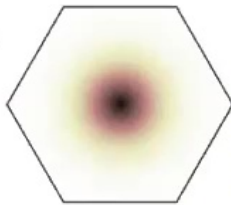
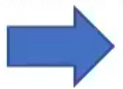
1a is AA-stacking region

We hence introduce trial Gaussian-type WFs, $|W'_{\alpha=1,2}\rangle \sim |p_x\rangle \pm i|p_y\rangle$ and computed $\sum_{\alpha} |\langle W'_{\alpha} | \psi_n(\mathbf{k}) \rangle|^2$ for each band

Large overlap \rightarrow **The flat bands at $\mathbf{k} \neq 0$ are almost the trial WFs**

Wannier90

$$\langle W'_{\alpha} | \psi_n(\mathbf{k}) \rangle$$



Maximally localized WFs

WFs are extremely localized:

1. Spread $\sim 0.2a_M$
2. Hopping between NN $\sim 0.1\text{meV}$

96% of the flat bands are contributed by the WFs

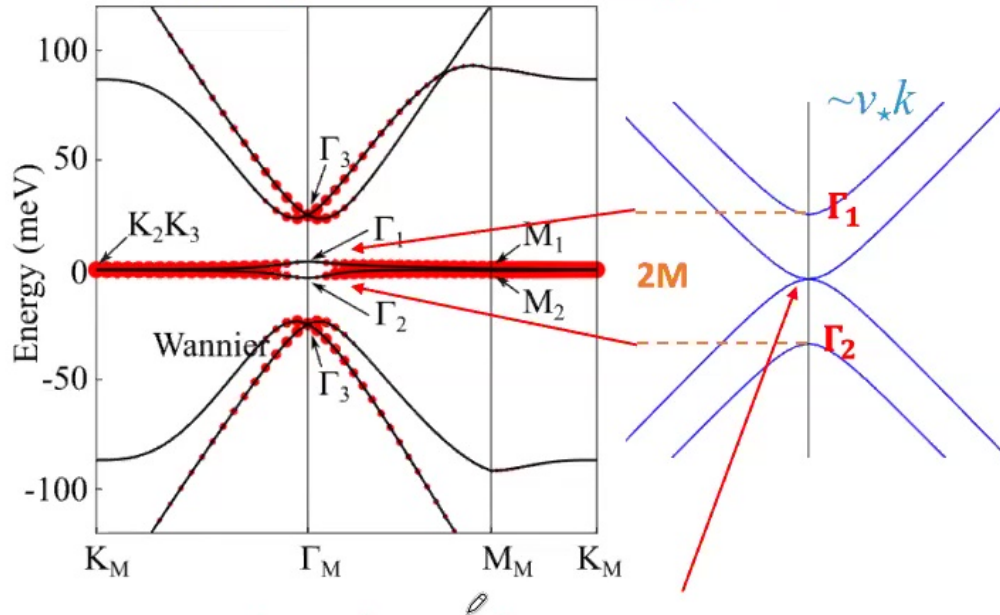
$$\frac{1}{2N} \sum_{kn} \sum_{R\alpha} |\langle W_{R\alpha} | \psi_n(\mathbf{k}) \rangle|^2 = 96\%$$

The correlation physics of flat bands must mainly come from these WFs!

$$\lambda_1 = \frac{1}{q_1} \sqrt{2 \log \frac{1-w_0^2}{w_1}}$$

Construction of the heavy fermion model

Our strategy: **Step II. Model the remaining 4% states**



The quadratic touching.

H^c has to be gapless: Since the WFs are trivial, H^c must have $4n+2$ ($n \in \mathbb{N}$) Dirac points due to the **symmetry anomaly**.

The quadratic touching is equivalent to two DPs.

$$H^c = P_c H^{BM} P_c, \quad P_c = 1 - P_f$$

We consider the lowest six bands

P_f contains Γ_3 at $k=0$

$\rightarrow P_c$ contains $\Gamma_3 + \Gamma_1 + \Gamma_2$

$$H^{(c,\eta)} = \begin{pmatrix} \Gamma_3 (L=\pm 1) & \Gamma_1 + \Gamma_2 (L=0) \\ \mathbf{0}_{2 \times 2} & v_*(\eta k_x \sigma_0 + i k_y \sigma_z) \\ v_*(\eta k_x \sigma_0 - i k_y \sigma_z) & M \sigma_x \end{pmatrix}$$

$\eta = \pm$ is the valley index

Determine the parameters:

$$H_{ab}^{(c,\eta)}(k) = \langle u_a^\eta(0) | H_{BM}^\eta(k) | u_b^\eta(0) \rangle \quad a,b=1 \dots 4$$

BM model, linear in $k \rightarrow H^{(c,\eta)}$ is linear in k

$$M=3.7\text{meV}$$

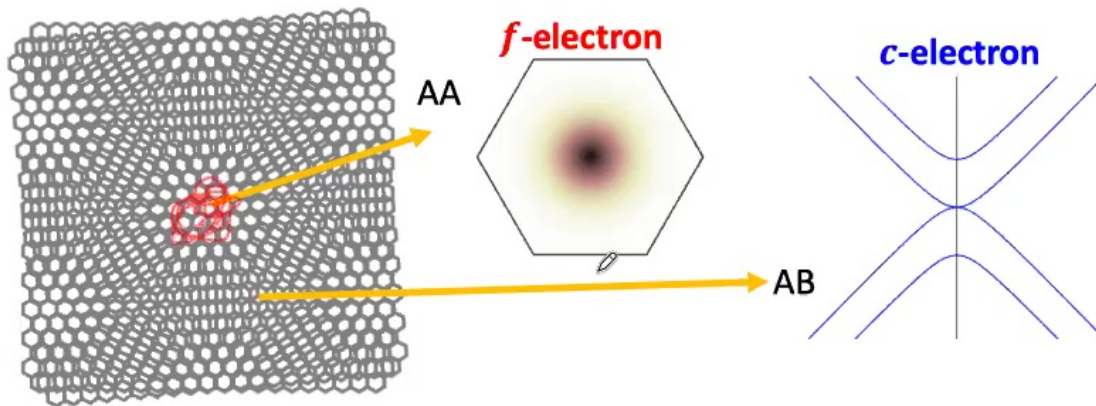
$$v_* = -4.3\text{eV} \cdot \text{\AA}$$

Construction of the heavy fermion model

Our strategy: **Step III. Couple the two parts**

$$\hat{H}_0 = \sum_{|\mathbf{k}| < \Lambda_c} \sum_{aa'\eta s} H_{aa'}^{(c,\eta)}(\mathbf{k}) c_{\mathbf{k}a\eta s}^\dagger c_{\mathbf{k}a'\eta s} + \frac{1}{\sqrt{N}} \sum_{\mathbf{R}} \sum_{\alpha a \eta s} \left(e^{i\mathbf{k}\cdot\mathbf{R} - \frac{|\mathbf{k}|^2 \lambda^2}{2}} H_{\alpha a}^{(fc,\eta)}(\mathbf{k}) f_{\mathbf{R}\alpha\eta s}^\dagger c_{\mathbf{k}a\eta s} + h.c. \right)$$

Λ_c : cutoff for the conduction band



Large enough $k \rightarrow$ decoupled
Only coupling around Gamma is relevant

	Reps	L
a=1,2 c-electrons	Γ_3	± 1
a=3,4 c-electrons	$\Gamma_1 + \Gamma_2$	0
$\alpha=1,2$ f-electrons	Γ_3	± 1

$$H^{(c,\eta)} = \begin{pmatrix} \mathbf{0}_{2 \times 2} & v_*(\eta k_x \sigma_0 + i k_y \sigma_z) \\ v_*(\eta k_x \sigma_0 - i k_y \sigma_z) & M \sigma_x \end{pmatrix} \quad H_a^{(cf,\eta)}(k) = \langle u_a^\eta(0) | H_{BM}(k) | v_\alpha^\eta(0) \rangle = \begin{pmatrix} \gamma + v'_*(\eta k_x \sigma_x + k_y \sigma_y) & \\ & \mathbf{0}_{2 \times 2} \end{pmatrix}$$

a=1...4 $\alpha = 1,2$

$$\gamma = -24.8 \text{ meV}; \quad v'_* = 1.6 \text{ eV} \cdot \text{\AA}$$

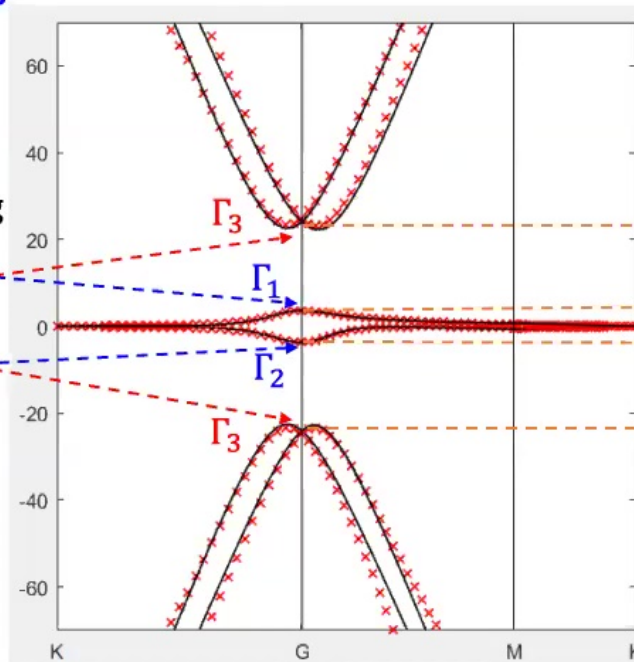
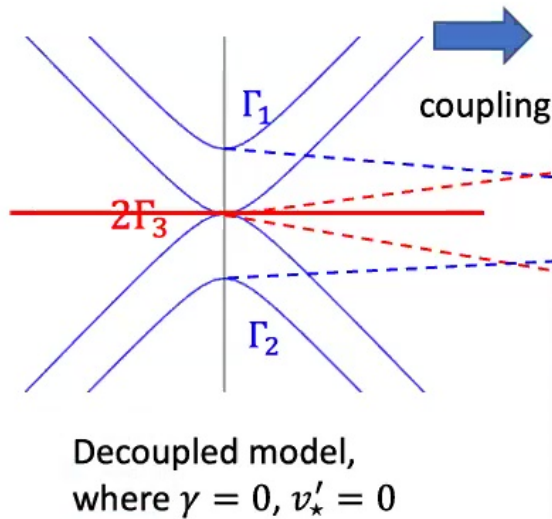
Construction of the heavy fermion model

Recover the BM model bands

For small k

$$H^\eta(k) = \left(\begin{array}{cc|cc} 0_{2 \times 2} & v_*(k_x \eta \sigma_0 + i k_y \sigma_z) & \gamma + v'_*(k_x \sigma_x + k_y \sigma_y) & \\ v_*(k_x \eta \sigma_0 - i k_y \sigma_z) & M \sigma_x & 0_{2 \times 2} & \\ \hline \gamma + v'_*(k_x \eta \sigma_x + k_y \sigma_y) & 0_{2 \times 2} & 0_{2 \times 2} & \end{array} \right)$$

f -orbitals (Γ_3) only couple to Γ_3 c-bands



red dots: BM model
black lines: our model

$2M$ determines the bandwidth of the flat bands

$\gamma = -24.8 \text{ meV}$
 $M = 3.7 \text{ meV}$

Hybridization γ is larger than bandwidth, but, as shown below, smaller than on-site repulsion

Interaction Hamiltonian

$$\hat{H}_I = \frac{1}{2} \int d^2\mathbf{r}_1 d^2\mathbf{r}_2 V(\mathbf{r}_1 - \mathbf{r}_2) : \hat{\rho}(\mathbf{r}_1) :: \hat{\rho}(\mathbf{r}_2) :$$

$$V(\mathbf{r}) = U_\xi \sum_{n=-\infty}^{\infty} \frac{(-1)^n}{\sqrt{(\mathbf{r}/\xi)^2 + n^2}}$$

$$:A := A - \langle G_0|A|G_0\rangle$$

G_0 is the normal state at charge neutrality point

$\rho \sim f^\dagger f + c^\dagger c + f^\dagger c + c^\dagger f \rightarrow$ Sixteen terms in $H_I \sim \rho \cdot V \cdot \rho$

$$\rightarrow H_I = H_U + H_V + H_W + H_J + H_{\bar{J}} + H_K$$

$H_U \sim f^\dagger f V f^\dagger f$: density-density for f

$H_V \sim c^\dagger c V c^\dagger c$: density-density for c

$H_W \sim c^\dagger c V f^\dagger f$: density-density between f and c

$H_J \sim f^\dagger c V c^\dagger f + h.c.$: exchange interaction

$c + h.c.$: double hybridization

$f + h.c.$: hybridization

On-site repulsion found to be the largest energy scale

Conserve particle number of f -electrons, commute with H_U

do not commute with H_U , are high energy processes, will be omitted in the current work.

- ✓ Automatic ⌘U
- Hidden ⌘I
- Arrow ⌘A
- Pen ⌘P
- Laser Pointer ⌘L
- Pen Color ▶
- Laser Color ▶

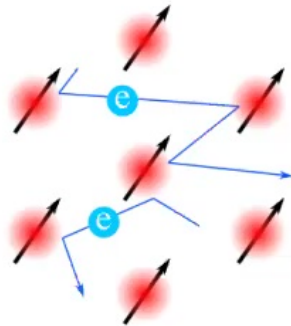
Interaction Hamiltonian

$$\hat{H}_I = \overset{H_U}{\frac{U_1}{2} \sum_{\mathbf{R}} : \rho_{\mathbf{R}}^f :: \rho_{\mathbf{R}}^f :} + \overset{H_V}{\int d^2\mathbf{r} d^2\mathbf{r}' : \rho^c(\mathbf{r}) : V(\mathbf{r} - \mathbf{r}') : \rho^c(\mathbf{r}') :} + \overset{H_W}{\sum_{\mathbf{R}a} \Omega_0 W_a : \rho_{\mathbf{R}}^f :: \rho_a^c(\mathbf{R}) :}$$

$$\overset{H_J}{- \frac{J}{2N} \sum_{\mathbf{R}} \sum_{\substack{\alpha_1 \eta_1 s_1 \\ \alpha_2 \eta_2 s_2}} \sum_{|\mathbf{k}_1|, |\mathbf{k}_2| < \Lambda_c} e^{i(\mathbf{k}_1 - \mathbf{k}_2) \cdot \mathbf{R}} (\eta_1 \eta_2 + (-1)^{\alpha_1 + \alpha_2}) : f_{\mathbf{R}\alpha_1 \eta_1 s_1}^\dagger f_{\mathbf{R}\alpha_2 \eta_2 s_2} :: c_{\mathbf{k}_2, \alpha_2 + 2, \eta_2 s_2}^\dagger c_{\mathbf{k}_1, \alpha_1 + 2, \eta_1 s_1} :}$$

U_1	W_1, W_2	W_3, W_4	J
57.94	44.03	50.02	16.38

in units of meV



U_1 : the main source of symmetry breaking

(> hybridization $\gamma = -24.75\text{meV}$)

(>> bandwidth $2M = 7.4\text{meV}$)

→ tend to freeze the charge fluctuation of f-electrons

→ leading to a local flat-U(4) moment

J : Ferromagnetic coupling between U(4)-moments (defined later)

V renormalize the parameters of Fermi-liquid formed by c

W : effective chemical potential for c -electrons

1. U(4) symmetries

Previous study

Kang2019PRL, Bultinck2020PRX, Bernevig2021PRB TBG-III

The two-band **projected Hamiltonian** was shown to have
 a **chiral-U(4)** symmetry if, $w_0 = 0, \{C, H\} = 0$
 a **flat-U(4)** symmetry if kinetic energy = 0
 a **U(4) × U(4)** symmetry when both are satisfied
 (shown in Song2021PRB TBG-II, $w_0=0$ is not a good approx.)

flat-U(4) only commute with the projected Hamiltonian, not the full Hamiltonian

Only know how the generators act in momentum space

In our model

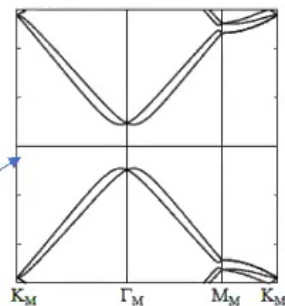
*U(4)'s commute with the FULL Hamiltonian
 U(4)'s have simple expressions in real space*

Flat limit $M=0$

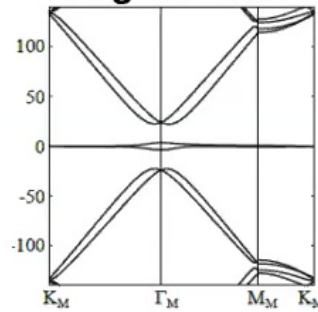
$$S = (-\sigma_0) \oplus \sigma_0 \oplus \sigma_0$$

→ Flat-U(4) symmetry

exact flat bands



Original band



First chiral limit $v'_* = 0$ ($w_0=0$)

$$C = (-\sigma_z) \oplus \sigma_z \oplus \sigma_z$$

→ Chiral-U(4) symmetry



1. U(4) symmetries

Flat-U(4) rotation matrices

$$\Sigma^{(\mu\nu,f)} = \{\sigma_0\tau_0s_\nu, \sigma_y\tau_x s_\nu, \sigma_y\tau_y s_\nu, \sigma_0\tau_z s_\nu\}$$

orbital
valley
spin

Commute with orbital angular momentum $\xi = \sigma_z\tau_z$

$$M = 0$$

Fundamental U(4)-reps [1]

$p_x + ip_y$	$p_x - ip_y$
$\xi = 1$	$\xi = -1$
1, +, \uparrow	2, +, \uparrow
1, +, \downarrow	2, +, \downarrow
2, -, \uparrow	1, -, \uparrow
2, -, \downarrow	1, -, \downarrow

H_I respects flat-U(4)

$$\hat{H}_I = \frac{U_1}{2} \sum_{\mathbf{R}} : \rho_{\mathbf{R}}^f :: \rho_{\mathbf{R}}^f : + \int d^2\mathbf{r} d^2\mathbf{r}' : \rho^c(\mathbf{r}) : V(\mathbf{r} - \mathbf{r}') : \rho^c(\mathbf{r}') : + \sum_{\mathbf{R}a} \Omega_0 W_a : \rho_{\mathbf{R}}^f :: \rho_a^c(\mathbf{R}) :$$

$$H_J - \frac{J}{2N} \sum_{\mathbf{R}} \sum_{\substack{\alpha_1 \eta_1 s_1 \\ \alpha_2 \eta_2 s_2}} \sum_{|\mathbf{k}_1|, |\mathbf{k}_2| < \Lambda_c} e^{i(\mathbf{k}_1 - \mathbf{k}_2) \cdot \mathbf{R}} (\eta_1 \eta_2 + (-1)^{\alpha_1 + \alpha_2}) : f_{\mathbf{R}\alpha_1 \eta_1 s_1}^\dagger f_{\mathbf{R}\alpha_2 \eta_2 s_2} :: c_{\mathbf{k}_2, \alpha_2 + 2, \eta_2 s_2}^\dagger c_{\mathbf{k}_1, \alpha_1 + 2, \eta_1 s_1} :$$

The density-density terms satisfy the flat-U(4) symmetries because the density operators are identity in each fundamental U(4) rep.

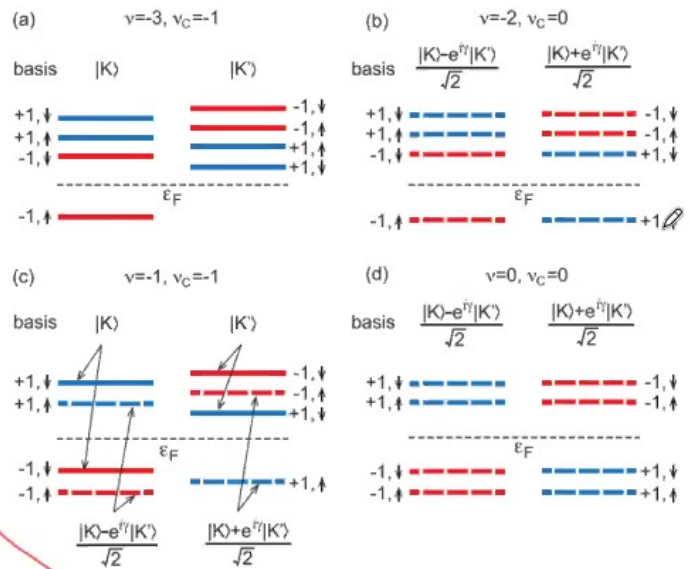
The exchange term: U(4) moment * U(4) moment

$$\hat{H}_J = -J \sum_{\mu\nu\xi} e^{-i\mathbf{q} \cdot \mathbf{R}} : \hat{\Sigma}_{\mu\nu}^{(f,\xi)}(\mathbf{R}) :: \hat{\Sigma}_{\mu\nu}^{(cf,\xi)}(\mathbf{q}) :$$

2-3. Ground states & excitations at integer fillings

Previous study

Ground states from *involved* numerical or perturbation calculation in *projected models*

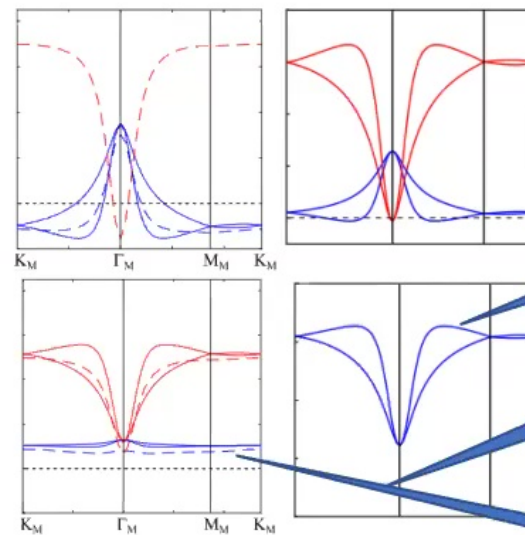


Bultinck2020PRX
Lian2021PRB
Kang2019PRL

Exact charge ± 1 excitations, *not understood*

Bernevig, Song2021PRB TBG-V

Kumar2021PRB, VafeekPRB2021, Khalaf-Arxiv2009.14827



Blue: particle
Red: hole

1. Dispersion is related to topology, but how?

2. What determines the gaps?

3. Flat bands?

In our model

Hund's-like rules are derived for ground states, as simple as a *few-level problem*

(1) Bandwidths, (2) gaps and (3) flat bands are *analytically derived*

2-3. Ground states & excitations: $\nu = 0$

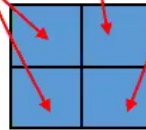
A trial state is at $\nu = 0$ $|\Psi_0\rangle = U \prod_{\mathbf{R}} f_{\mathbf{R}1+\uparrow}^\dagger f_{\mathbf{R}1+\downarrow}^\dagger f_{\mathbf{R}2+\uparrow}^\dagger f_{\mathbf{R}2+\downarrow}^\dagger |FS\rangle$

A U(4) rotation operator

For $U = 1$, Ψ_0 is parent state of the valley polarized (VP) state

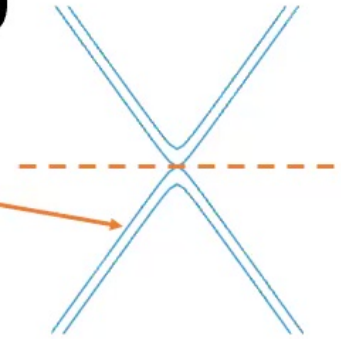
All Ψ_0 should be degenerate when $M = 0$ because of flat-U(4)

They form the U(4) representation [2,2] :



$\xi = + \quad -$

The (gapless) Fermi sea state occupying the lower c-bands



highest, where U(4) indices are mostly symmetric under exchange

- Should be more favored than other reps due to **Hund's rule**
- Also confirmed in numeric.

For $U = e^{-i\frac{\pi}{2}\hat{\Sigma}_{x0}}$, Ψ_0 is parent state of the Kramer valley coherent state (K-IVC)

$$\prod_{\mathbf{R}} \frac{1}{4} (f_{\mathbf{R}1+\uparrow}^\dagger + f_{\mathbf{R}2-\uparrow}^\dagger) (f_{\mathbf{R}1+\downarrow}^\dagger + f_{\mathbf{R}2-\downarrow}^\dagger) (-f_{\mathbf{R}1-\uparrow}^\dagger + f_{\mathbf{R}2+\uparrow}^\dagger) (-f_{\mathbf{R}1-\downarrow}^\dagger + f_{\mathbf{R}2+\downarrow}^\dagger) |FS\rangle$$

$T = \tau_x K$ is broken, $T' = e^{i\pi \hat{\Sigma}_{x0}^f} T = i\sigma_y \tau_x T = i\sigma_y K$ is respected

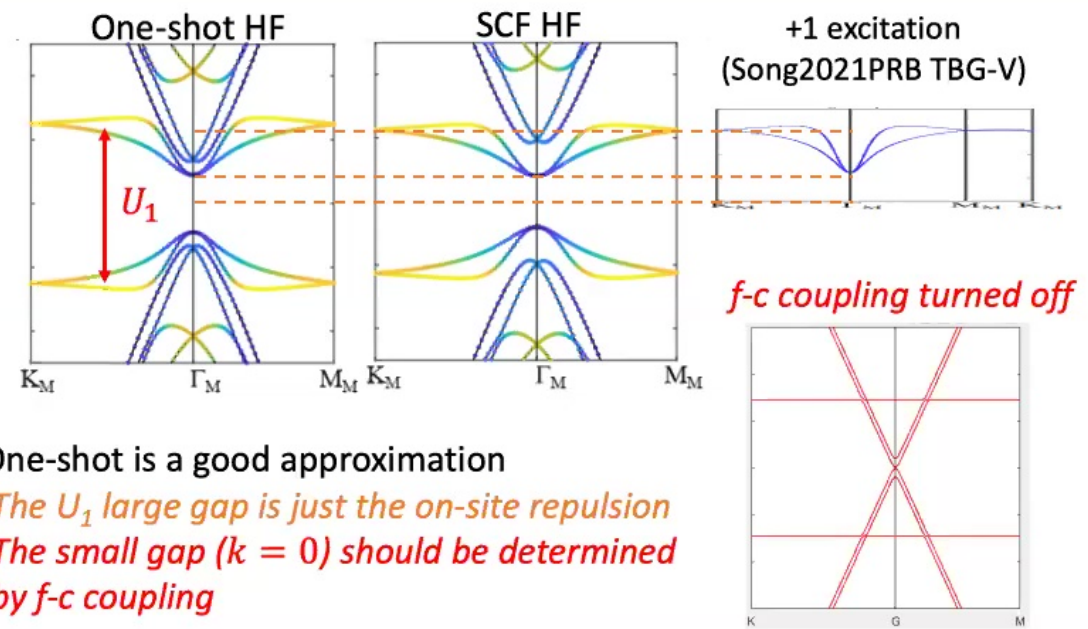
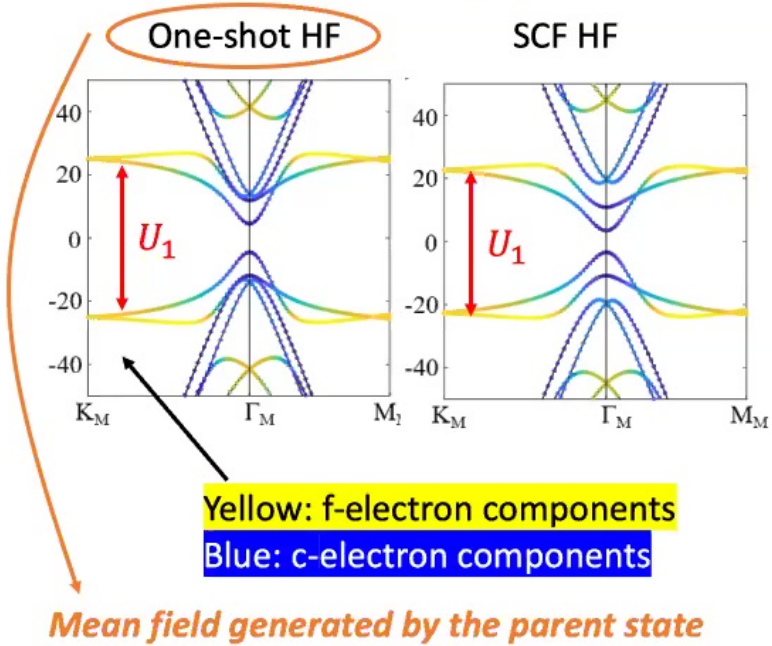
$\langle f^+ c \rangle = 0$. Hybridizations are needed to minimize the total energy.

2-3. Ground states & excitations: $\nu = 0$

Hartree-Fock (HF) with *initial condition* given by the *parent states*

Valley polarized (VP)

Kramer valley coherent state (K-IVC)



- One-shot is a good approximation
1. The U_1 large gap is just the on-site repulsion
 2. The small gap ($k = 0$) should be determined by f-c coupling

→ Larger Gap = Lower Total Energy
K-IVC is favored

$$E = \left(\sum_{k,n \in occ} E_{k,n} \right) - \langle H_I \rangle$$

Interaction energy
(same for U4-related states)

Quasi-particle energy

2-3. Ground states & excitations: $\nu = 0$

One-shot mean field Hamiltonian at Γ_M :

$M=0$

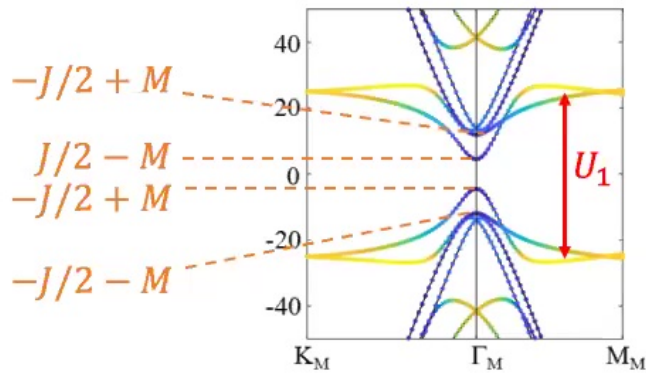
$$\bar{H}(k \rightarrow 0) = \begin{pmatrix} 0_{4 \times 4} & 0_{4 \times 4} & \gamma \\ 0_{4 \times 4} & M\sigma_x - J(\tau_z \bar{O}^{fT} \tau_z + \sigma_z \bar{O}^{fT} \sigma_z) & 0_{4 \times 4} \\ \gamma & 0_{4 \times 4} & -U_1 \bar{O}^{fT} \end{pmatrix}$$

$\bar{O}^f = \langle f^\dagger f \rangle - \frac{1}{2}$ is density matrix of the trial state

Γ_3 from c-bands
 $\Gamma_1 + \Gamma_2$ from c-bands
 Γ_3 from f-bands

VP $\bar{O}^f = \frac{1}{2} \sigma_0 \tau_z \zeta_0$

$$M\sigma_x - \frac{J}{2} \tau_z$$

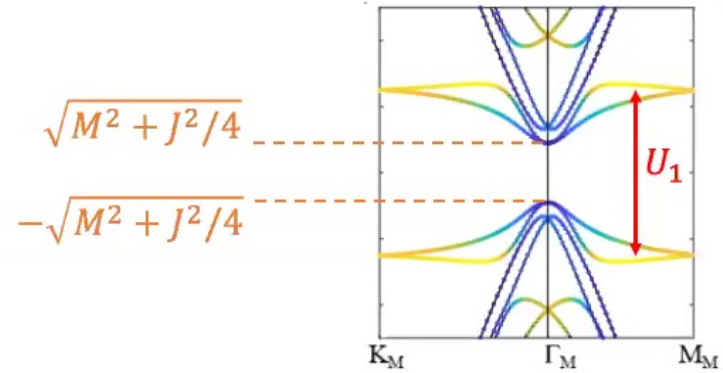


Gap = $|J - 2M|$
 Bandwidth = $U_1/2 - |J/2 - M|$

Rotation $e^{i\frac{\pi}{4} \sigma_y \tau_x}$

K-IVC $\bar{O}^f = \frac{1}{2} \sigma_y \tau_y \zeta_0$

$$M\sigma_x - \frac{J}{2} \tau_y \sigma_y$$



Gap = $\sqrt{J^2 + 4M^2}$
 Bandwidth = $U_1/2 - \sqrt{J^2/4 + M^2}$

2-3. Ground states: general rules

1. (Hund's rule) The f -electrons form the highest weight $U(4)$ -rep they can access, to save **Coulomb energy** ✓

2. O^f is rotated by $U(4)$ such that it minimizes the **quasi-particle energy**, which can be estimated as energies of the occupied $\Gamma_1 + \Gamma_2$ levels from

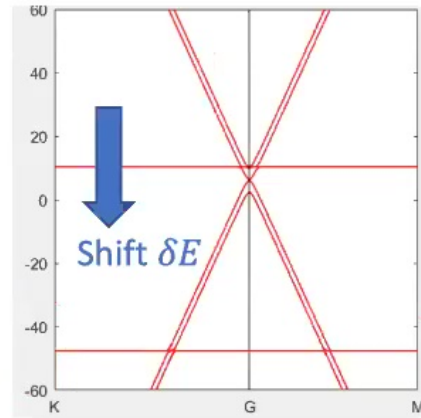
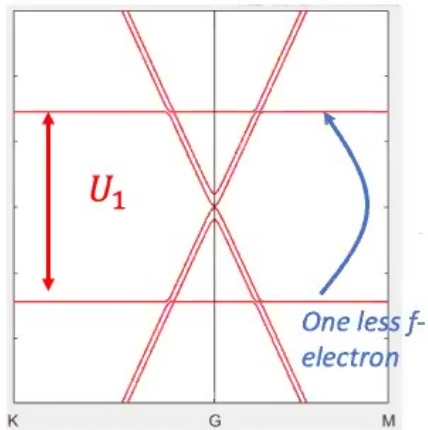
$$M\sigma_x - J(\tau_z \bar{O}^{fT} \tau_z + \sigma_z \bar{O}^{fT} \sigma_z)$$

Here we only look at the $\Gamma_1 + \Gamma_2$ c -electron block because they are always closest to Fermi level, in agreement with previous studies where Γ_3 states are omitted

Consistent with the numerical results

2-3. Excitations: $\nu = -1$

$\nu = 0 \rightarrow \nu = -1$

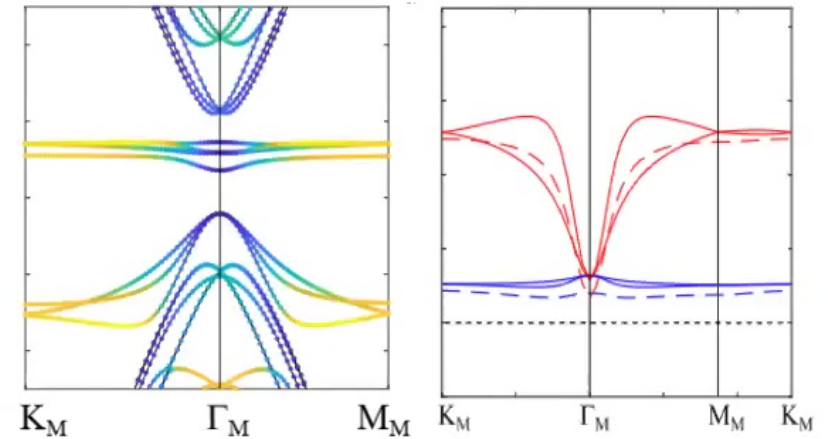


Relative shift between *f*- and *c*-bands (through Hartree channel)

ΔE turns out to be $\frac{U_1}{2}$ at $\nu = -1$

Coupling

Flat bands explained



Consistent with results in Bernevig, Song2021PRB

f-c coupling turned off



4. Topology

arXiv2111.05865

Previous studies: $C = \pm 1$ at $|v| = 1, 3$

Bultinck et al. 2020PRX,
Lian et al. 2021PRB,
Liu et al. 2019PRX

In our model:

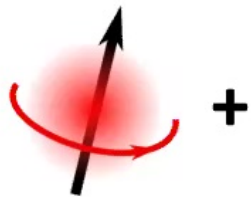
Local moments gap the quadratic touching point

$$(k_x^2 - k_y^2)\sigma_x + 2k_x k_y \sigma_y + \mathbf{F} \sigma_z$$

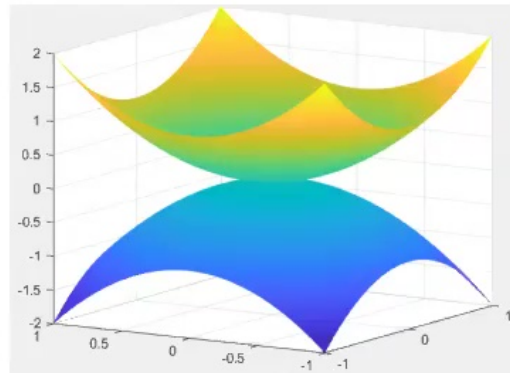
from the coupling between f and c
 $\sim \mathbf{J} \cdot \mathbf{O}^f$

$$C = - \sum_{\alpha\eta s} \eta (-1)^{\alpha-1} n_{\alpha\eta s}$$

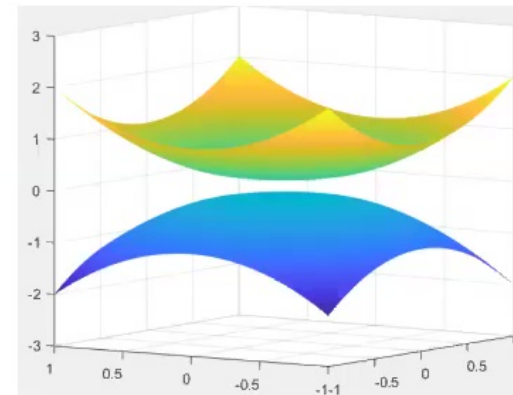
Angular momentum of $f_{\alpha\eta s}$ (points to $\eta (-1)^{\alpha-1}$)
Occupation of $f_{\alpha\eta s}$ (points to $n_{\alpha\eta s}$)



+



→




$C = \pm 1$

- **Construction of our model**

- **New understanding of correlated states**

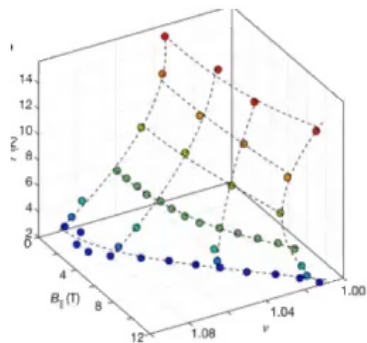
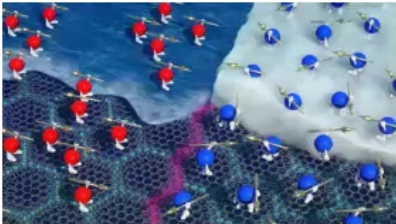
- **Insight into new physics**

- 
1. *Local moments & Kondo Physics*
 2. *Superconductivity*
 3. *Correlation under magnetic field*

Local moments at $\nu = -1$

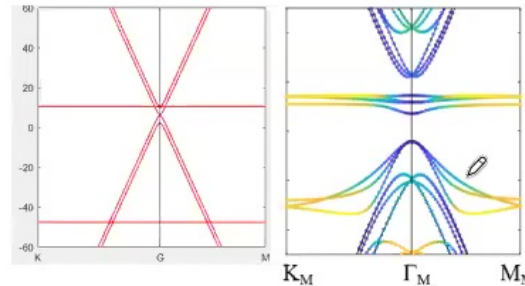
Pomeranchuk effect

large entropy in the ordered phase, which disappear under magnetic field
 → loosely coupled local moments



Low T: liquid
 High T: *barely coupled moments*

Insight from the heavy fermion model



Smallest Fermi surface

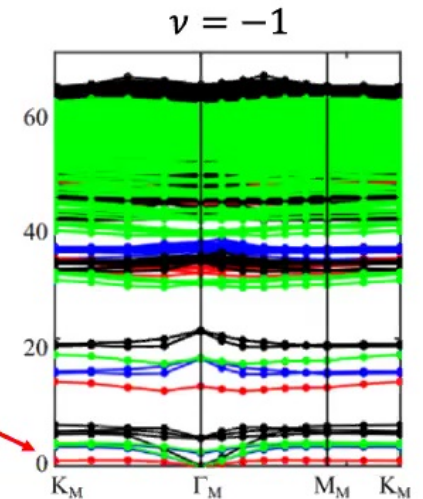
- *a minimal coupling* between local moments & c-bands
- Weak coupling between moments

Weak coupling is reflected as

- (i) Energy of second lowest (HF) state is just 0.003meV above the ground state
- (ii) Extremely low energy flat Goldstone modes

All these indicate that the *local moments* are (very) loosely coupled

Should be similar to *Kondo Physics*



Obtained in Song2021PRB (TBG-V)

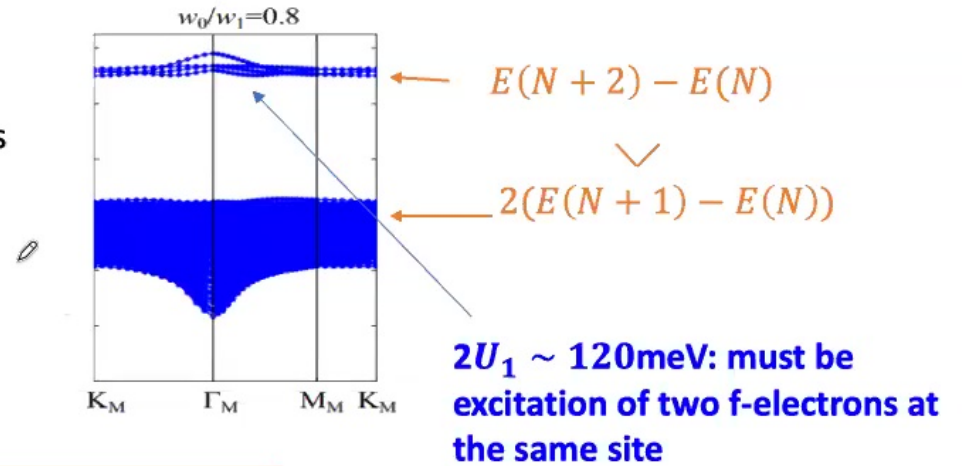
Discussion: Superconductivity

Absence of pairing (around all integer fillings) in the flat-band-projected model

The projected model is positive semidefinite if kinetic energy is discarded →

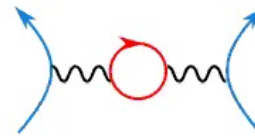
Then the binding energy for cooper pair
 $\Delta = E(N + 2) + E(N) - 2E(N + 1)$
 is proven to be positive in Song2021PRB (TBG-V)

Charge 2 excitations (Bernevig, Song2021PRB TBG-V)



Now the kinetic energy is unbounded (due to anomaly) → SC is possible

Potential mechanism I: U(4)-spin-wave as SC glue



Potential mechanism II: charge fluctuation
 the omitted term $H_{\bar{j}} \sim f^+ f^+ c c + h.c.$ may become important in SC.
 A second order perturbation gives

$$\delta H \propto - \frac{c^+ c^+ \overbrace{f f f}^{\boxed{f f f}} f^+ c c}{U_1} + h.c.$$

U_1 : from on-site repulsion

If f-electrons are ordered, these can be replaced by expectations

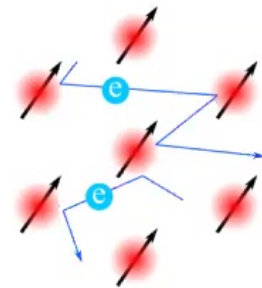
Now must be coupled to conduction bands

Is topological flat-band the answer to the contradictory?

A phenomenological model would consist of both local moments & itinerant electrons

topology \rightarrow delocalized wave function

flatness \rightarrow "localization"?



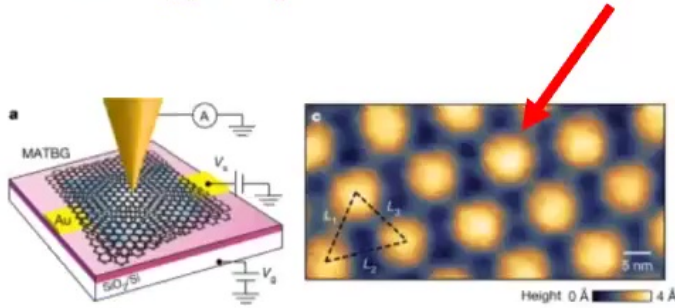
relation?

Heavy Fermion Physics?

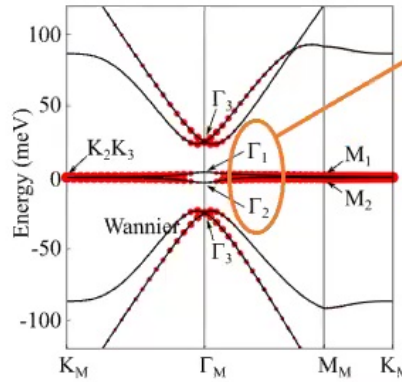


Construction of the heavy fermion model

Our strategy: Step I. Where does the local states come from?



Xie2019, Choi2019, Kerelsky2019, Jiang2019, Wong2020



Suppose we can replace $\Gamma_1 + \Gamma_2$ by Γ_3 , then flat bands match p_x, p_y orbitals at triangular lattice

Wyckoff pos.	1a (000)		
Site sym.	$6'22', 32$		
EBR	$[A_1]_a \uparrow G$	$[A_2]_a \uparrow G$	$[E]_a \uparrow G$
Orbitals	s	p_z	p_x, p_y
$\Gamma (000)$	Γ_1	Γ_2	Γ_3
$K (\frac{1}{3} \frac{1}{3} 0)$	K_1	K_1	$K_2 K_3$
$M (\frac{1}{2} 00)$	M_1	M_2	$M_1 \oplus M_2$

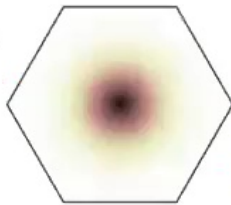
1a is AA-stacking region

We hence introduce trial Gaussian-type WFs, $|W'_{\alpha=1,2}\rangle \sim |p_x\rangle \pm i|p_y\rangle$ and computed $\sum_{\alpha} |\langle W'_{\alpha} | \psi_n(\mathbf{k}) \rangle|^2$ for each band

Large overlap \rightarrow The flat bands at $\mathbf{k} \neq 0$ are almost the trial WFs

96% of the flat bands are contributed by the WFs

$\langle W'_{\alpha} | \psi_n(\mathbf{k}) \rangle$ \rightarrow Wannier90



WFs are extremely localized:

1. Spread $\sim 0.2a_M$
2. Hopping between NN $\sim 0.1\text{meV}$

$$\frac{1}{2N} \sum_{\mathbf{k}n} \sum_{R\alpha} |\langle W_{R\alpha} | \psi_n(\mathbf{k}) \rangle|^2 = 96\%$$

$$\lambda_1 = \frac{1}{q_1} \sqrt{2 \log \frac{1-w_0^2}{w_1}}$$

Maximally localized WFs

The correlation physics of flat bands must mainly come from these WFs!